Changes in the chemical and dynamic properties of cardiac troponin T cause discrete cardiomyopathies in transgenic mice

Briar R. Ertz-Berger*†, Huamei He‡, Candice Dowell*, Stephen M. Factor†§, Todd E. Haim*, Sara Nunez*, Steven D. Schwartz*, Joanne S. Ingwall‡, and Jil C. Tardiff*†¶

Departments of *Physiology and Biophysics, †Medicine, and §Pathology, Albert Einstein College of Medicine, Bronx, NY 10461; and ‡NMR Laboratory for Physiological Chemistry, Division of Cardiovascular Medicine, Department of Medicine, Brigham and Women's Hospital, Harvard Medical School, Boston, MA 02115

Communicated by Dominick P. Purpura, Albert Einstein College of Medicine, Bronx, NY, October 20, 2005 (received for review June 28, 2005)

Cardiac troponin T (cTnT) is a central component of the regulatory thin filament. Mutations in cTnT have been linked to severe forms of familial hypertrophic cardiomyopathy. A mutational "hotspot" that leads to distinct clinical phenotypes has been identified at codon 92. Although the basic functional and structural roles of cTnT in modulating contractility are relatively well understood, the mechanisms that link point mutations in cTnT to the development of this complex cardiomyopathy are unknown. To address this question, we have taken a highly interdisciplinary approach by first determining the effects of the residue 92 mutations on the molecular flexibility and stability of cTnT by means of molecular dynamics simulations. To test whether the predicted alterations in thin filament structure could lead to distinct cardiomyopathies *in vivo*, we developed transgenic mouse models expressing either the Arg-92-Trp or Arg-92-Leu cTnT proteins in the heart. Characterization of these models at the cellular and whole-heart levels has revealed mutation-specific early alterations in transcriptional activation that result in distinct pathways of ventricular remodeling and contractile performance. Thus, our computational and experimental results show that changes in thin filament structure caused by single amino acid substitutions lead to differences in the biophysical properties of cTnT and alter disease pathogenesis.

contractility | molecular dynamics | thin filament | familial hypertrophic cardiomyopathy

The regulatory function of the cardiac sarcomere resides in the thin filament. Muscle contraction depends on the access of the myosin head to the actin filament, which is regulated by a cascade of allosteric changes in the interactions of the proteins within the troponin [cardiac troponin T (cTnT), cTnI, and cTnC] and tropomyosin–actin complexes upon the binding of Ca^{2+} (1, 2). Disruption of these important protein–protein interactions by many naturally occurring thin filament mutations is poorly tolerated. Many mutations in cTnT result in a severe form of genetic cardiomyopathy, familial hypertrophic cardiomyopathy (FHC). FHC caused by cTnT mutations is characterized by a high frequency of early sudden cardiac death, often in the absence of overt ventricular hypertrophy (3). The direct link between mutations in the structural components of the cardiac sarcomere and the resultant complex clinical phenotype remains unknown.

cTnT is a highly elongated protein that interacts with all other components of the thin filament and has been described as the "glue" of the contractile regulatory system (1). Codon 92 in cTnT is a mutational "hotspot," and patients carrying each of the three predicted missense mutations have been identified and exhibit distinct clinical phenotypes (4–6). Patients carrying the Arg-92-Trp (R92W) missense mutation in cTnT develop mild or no ventricular hypertrophy, yet they experience a high frequency of early cardiac sudden death (7). In contrast, although carriers of the Arg-92-Leu (R92L) mutation often exhibit ventricular hypertrophy and eventually develop cardiac failure, the frequency of sudden death is relatively low (4). We hypothesize that these disparate clinical phenotypes are, in part, due to specific alterations in the multiple protein–protein interactions modulated by cTnT within the regulatory thin filament.

Residue 92 flanks the Ca^{2+}-independent tropomyosin-binding domain near the N terminus of cTnT. Recent biophysical and biochemical studies from several laboratories have shown that this domain plays a central role in modulating the protein–protein interactions between the thin filament and myosin during a normal contractile cycle (8, 9). Approximately 65% of the known cTnT mutations fall within or immediately flank the N-terminal tail domain, and several have been shown to alter both cTnT flexibility and the stability of the TnT–tropomyosin interaction (8, 10, 11). Of note, the R92Q, R92W, and R92L cTnT mutations have different effects on the stability of the TnT–tropomyosin complex *in vitro* (10, 12, 13). The clinical variability among patients with residue 92 mutations, coupled with the observed alterations in *in vitro* thin filament regulation, suggests that even subtle changes in cTnT function (caused by amino acid substitutions at the same residue) are sufficient to cause distinct cardiomyopathies.

To address the central question of how single amino acid substitutions in cTnT can result in independent cardiomyopathies, in the present study, we have used a highly integrative approach that combines molecular computational methodologies with our ability to engineer closely related transgenic mice expressing mutant cTnT proteins in the heart. The work reported here shows that the R92W and R92L mutations alter the dynamic and biochemical properties of murine cTnT and that these changes lead to early activation of distinct signaling pathways that govern myocellular growth and ultimately lead to pathogenic cardiovascular remodeling.

Materials and Methods

Molecular Dynamics (MD) Simulations. The commercial software program INSIGHTII (Accelrys, Inc., San Diego) was used to build the initial α-helix models corresponding to the WT/nontransgenic (NT), R92L, and R92W mutants of the 101-aa murine cTnT sequence, corresponding to residues 70–170. Minimization of each model was performed with the CHARMM22 macromolecular simulation package with a classical potential for all atoms, using the steepest-descent method for 20,000 cycles and a step size of 0.2 Å or until the gradient of the energy converged (14). For the nonbonding interactions, we calculated the energy contributions for

Conflict of interest statement: No conflicts declared.

Freely available online through the PNAS open access option.

Abbreviations: cTnT, cardiac troponin T; FHC, familial hypertrophic cardiomyopathy; MD, molecular dynamics; NT, nontransgenic; ANF, atrial natriuetic factor; αSK, α-skeletal actin; MCIP1, modulatory calcineurin-interacting protein 1; LVSP, left ventricular systolic pressure.

¶To whom correspondence should be addressed at: Department of Physiology and Biophysics, Albert Einstein College of Medicine, 1300 Morris Park Avenue, Bronx, NY 10461. E-mail: tardiff@aecom.yu.edu.

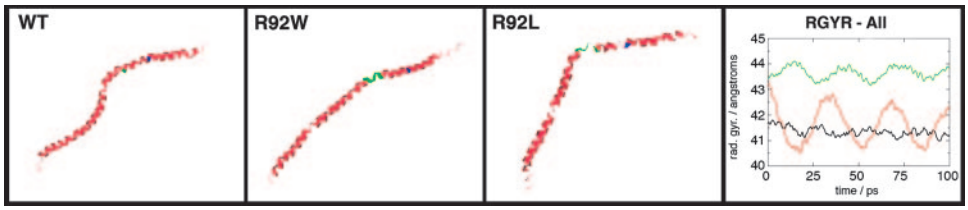

Fig. 1. Structural modeling of murine cTnT and generation of residue 92 transgenic mice. Mutation-specific alterations in the secondary structure of the 101-aa sequence of mouse cTnT corresponding to amino acids 70–170. ''Hinge'' residues 104–108 are shown in green, and residue R92 is shown in blue. The rightmost panel shows the radius of gyration as a function of time during the simulation. Black, WT; red, R92L; green, R92W.

pairs of atoms within a cutoff of 12 Å and used a smoothing function to gradually reduce to zero this contribution between 12 and 14 Å. These minimized structures were the starting models. MD runs were performed for each model with a time step of integration of 1 fs. Initial velocities were assigned based on a Gaussian distribution at a low temperature. A constant dielectric of 4 was used to simulate the protein environment. We used the same nonbonding interactions as for the minimization. The SHAKE algorithm was used to constrain all bonds involving hydrogen atoms. After an initial heating phase of 10 ps during which the temperature was slowly increased from 0 to 300 K, we allowed the systems to equilibrate for 50 ps at 300 K, rescaling the velocities every 100 steps to the 300-K target temperature, using the same scaling factor for all atoms in the three models. We continued the simulation for another 100 ps, during which we collected the coordinates every 5 fs for each model (WT, R92L, and R92W) and monitored properties of the system.

Residue 92 Hotspot Transgenic Mice. The R92W and R92L constructs were generated by means of oligonucleotide mutagenesis as described in ref. 15. The WT (*c-myc* tag control line) is described in ref. 16. To ensure a uniform genetic background, the two isolated 50:50 transgenic:endogenous cTnT mice were subsequently backcrossed to unrelated C57/BL6 animals for at least six generations.

Light and Ultrastructural Tissue Analysis. Tissue sections for sarcomeric ultrastructural analysis were isolated, fixed, and stained with uranyl acetate and lead citrate and examined with a JEOL-100CX electron microscope as described in ref. 15. Histological analysis was performed on tissue sections from 6-month-old male mice. Both ultrastructural and light microscopic evaluation was performed in a blinded fashion.

Transcript Analysis. Isolation of total RNA from mouse hearts and Northern blot analysis was performed as described in ref. 15. Resultant blots were hybridized with a series of radiolabeled DNA probes representing atrial natriuetic factor (ANF), α-skeletal actin (αSK), modulatory calcineurin-interacting protein 1 (MCIP1), SERCA2a [sarco(endo)plasmic reticulum calcium ATPase 2a], phospholamban, and GAPDH. Quantitation was performed on three independent sets of blots by PhosphorImager exposure and analysis with IMAGEQUANT 5.0 software (Amersham Pharmacia Biosciences). One-way ANOVA with Tukey's posttest was used to evaluate differences between the transgenic and NT lines within each time point. A level of $P < 0.05$ was accepted as statistically significant.

Adult Murine Ventricular Myocyte Isolation, Confocal Analysis, and Cell Size Determination. Ventricular myocytes were dissociated from 6-month-old mice as described by Nagata *et al.* (17). For transgene protein localization, cells were affixed to laminin-coated coverslips and incubated with either JLT-12 mAb (Sigma) at a dilution of 1:50 (NT) or *c-myc* epitope mAb 9E10.2 (Santa Cruz Biotechnology) at 1:1,000 (WT, R92W, and R92L). Coverslips were then incubated with Cy2 (Molecular Probes) at 1:100 and mounted on glass slides for imaging with a Leica TCS SP2 AOBS confocal microscope with $\times$60 oil immersion optics. A separate aliquot of myocytes was used for cell size determinations. All rectangular myocytes with striations were recorded on videotape. The myocytes with unobstructed edges were measured in their relaxed state by using video edge detection (IONWIZARD SOFTEDGE, IonOptix, Milton, MA), and surface area was calculated (length $\times$ width); n values were derived from three independent hearts per line. A Student t test was used to evaluate differences between the transgenic line and the corresponding controls for each individual parameter. A level of $P < 0.05$ was accepted as statistically significant.

Isolated Heart Preparations and Contractile Performance. Hearts were isolated from R92W, R92L, and NT sibling mice and perfused in the Langendorff mode paced at 420 beats per minute (18). Isovolumic contractile performance data were measured under baseline perfusion conditions (perfusate $[Ca^{2+}]$ of 2.5 mM). For the $[Ca^{2+}]$-response experiments, the perfusate was switched to a low $[Ca^{2+}]$ of 1.5 mM; then, perfusate $[Ca^{2+}]$ was increased in 0.5 or 1.0 mM steps to a final $[Ca^{2+}]$ of 4 mM by infusing a 50 mM $CaCl_2$ stock solution through a side tubing driven by a digital console driver at 1–3% of coronary flow rate. Functional measurements were made when a new steady state was achieved ($\approx$2 min). Measures of systolic performance were left ventricular systolic pressure (LVSP) and $+dP/dt$; measures of diastolic performance were end-diastolic pressure and $-dP/dt$. Results are expressed as mean $\pm$ SEM. Factorial ANOVA was used to compare the NT and transgenic hearts.

Results

Independent Amino Acid Substitutions at Residue 92 of cTnT Alter Peptide Dynamics. To test whether the FHC-related R92W and R92L substitutions would alter TnT flexibility in murine cTnT, we performed MD simulations on a peptide containing residues 70–170; representative structures are shown in Fig. 1. The simulations demonstrate two mutation-related differences (the MD simulations are shown in Movies 1–3, which are published as supporting information on the PNAS web site). First, both mutant peptides show a pronounced hinge motion in the region of residue 104. This motion is quantitated as the time dependence in the simulation of the radius of gyration of the peptides (Fig. 1, rightmost panel). The WT peptide has little motion, whereas peptides with R92W and R92L substitutions show marked oscillations caused by the hinge motion. The related human mutation R92Q in cTnT has previously been shown to weaken the folding and stability of a similar human cTnT peptide; thus, even remote mutations can affect hinge motions (11). The other property revealed in the simulation is an unfolding of the helical structure in the R92L mutant. Results of a previous study suggested that the R92L mutation either increased helical stability or changed the propensity of the peptide to aggregate (10). Our computational results are compatible with decreased helical stability for both R92W and R92L peptides.

Both R92W-cTnT and R92L-cTnT Are Expressed and Incorporate into Native Sarcomeres *in Vivo*. To determine whether R92 mutations in cTnT could cause distinct cardiomyopathies and thus establish a

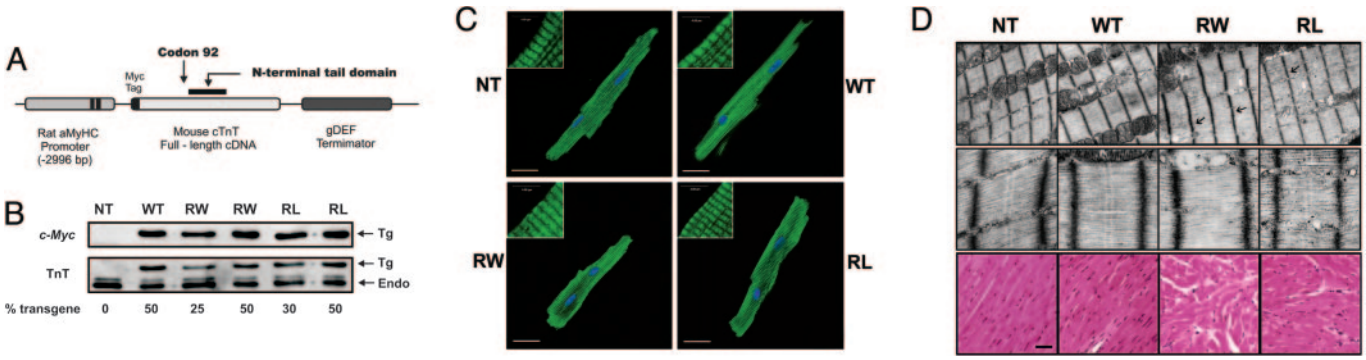

Fig. 2. Generation and characterization of mutant residue 92 mice. (*A*) Transgenic construct. (*B*) Identical Western blots of whole-heart homogenates were probed with *c-myc* (Tg) or cTnT mAb (Tg and Endo). Arrows correspond to the specific lines used in this study. (*C*) Immunostaining of adult ventricular myocytes isolated from all four lines and probed with either cTnT (NT) or *c-myc* (WT, R92W, and R92L) mAbs. (Scale bars: *C*, 20 μm; *Insets*, 4 μm.) (*D*) Isolated myofilament lysis and discontinuity (black arrows) were found in both R92W and R92L sections (R92W $\gg$ R92L). Dilated sarcomeric reticulum was found in the R92W sections (white arrows). Histopathology: R92W hearts exhibit a more severe cardiomyopathy. (Magnification: *Top*, $\times$30,000; *Middle*, $\times$120,000.) (Scale bar, 10 μm.)

biophysical basis for the observed human phenotypes, we developed two unique transgenic models expressing either R92W or R92L cTnT proteins in the murine heart; the transgene construct is shown in Fig. 2*A*. To detect the transgene product against the background of the endogenous murine WT cTnT, an 11-aa *c-myc* epitope was added to the N terminus and an independent nonmutant cTnT transgenic line established to control for the presence of the tag (WT). We have previously shown that cardiac histopathology, calcium sensitivity, contractility, and energetics are not changed by the presence of the *c-myc* tag alone (15, 18, 19). Ten independent transgenic lines were generated per construct. To approximate the expected 50:50 (mutant to WT) cTnT human FHC ratio, the present studies were performed by using the R92W and R92L lines that expressed a 50:50 ratio of transgenic to endogenous cTnT (Fig. 2*B*). Note that the down-regulation of the endogenous cTnT in response to the increase in expression of the cTnT transgene represents a replacement of the endogenous cTnT, not an overexpression of the transgene. Given that the N-terminal tail region of cTnT is involved in multiple thin filament protein–protein interactions and that both R92W and R92L cTnT exhibit a significant decrease in binding affinity for tropomyosin, we first determined whether the mutant cTnT proteins were capable of incorporating into native sarcomeres (10, 20). Adult ventricular myocytes isolated from WT, R92W, and R92L mice exhibited normal sarcomeric thin filament staining patterns (Fig. 2*C*).

Mutation-Specific Alterations in Cardiac Histopathology and Ultrastructure in R92 Mutant Mice. To determine whether the incorporation of either R92W or R92L cTnT directly led to myofibrillar disruption, we examined ultrastructure of left ventricular tissue from 6-month-old R92W and R92L mice. Both lines exhibited modest mutation-specific abnormalities (Fig. 2*D Top*). Although sections from both R92L and R92W were notable for prominent sarcoplasmic reticulum structures, only R92W mice exhibited mild degrees of myofibrillar lysis and prominent ANF granules. No sarcomere loss or destruction, mitochondrial abnormalities, or apoptotic nuclei were observed. Thus, there is no evidence for substantial sarcomere breakdown in R92 mice. Light microscopic analysis of ventricular sections from both R92W and R92L adult mice (Fig. 2D *Bottom*) revealed a broad range of histopathology consistent with that found in human mutant cTnT hearts, including myocyte disarray and degeneration, mild inflammatory cell infiltration, occasional hypertrophied cells, and minimal fibrosis (21). Hearts from R92W animals exhibited a more widespread histopathology that was first detectable at 2 months of age.

R92W Mice Alone Exhibit a Significant Decrease in Myocyte Size That Results in a Decrease in Ventricular Mass. A consistent finding among all previously published mutant cTnT murine models has been a decrease in ventricular mass (15, 16, 22). Examination of 6-month-old hearts from male NT, WT, R92W, and R92L animals revealed that although ventricular mass was decreased by 14% in R92W mice, there was a small (8–9%) increase in ventricular mass for hearts from the R92L mice compared with either NT or WT (Fig. 3*A*). Measurement of adult ventricular myocyte surface area made by using a similar matched set of hearts revealed that the alterations in ventricular mass are a direct result of nearly identical changes in myocyte size (Fig. 3*B*). Single myocyte video images are shown in Fig. 6, which is published as supporting information on the PNAS web site. These results suggest that amino acid substitutions at residue 92 leading to alterations in the flexibility of the N-terminal tail region of cTnT are sufficient to differentially alter early cardiomyocyte growth and, ultimately, ventricular mass.

Mutation-Specific Alterations in Contractile Performance. To determine whether amino acid substitutions at residue 92 in cTnT could cause mutation-specific alterations in either diastolic or systolic contractile performance, we measured isovolumic contractile performance under two conditions: at baseline and when challenged to increase work by increasing perfusate [Ca^{2+}] in 4- to 6-month-old mice (Fig. 4). The ability of the heart to increase work in response to inotropic agents such as Ca^{2+} is referred to as contractile reserve. Although both R92W and R92L hearts demonstrated impaired systolic performance (assessed both as LVSP and +dP/dt) both at baseline and with inotropic challenge, systolic dysfunction was more pronounced in the R92W hearts (Fig. 4 *A* and *B*). Diastolic function (assessed by both increases in end-diastolic pressure and decreases in the rate of relaxation, −dP/dt) was also impaired in both mutant

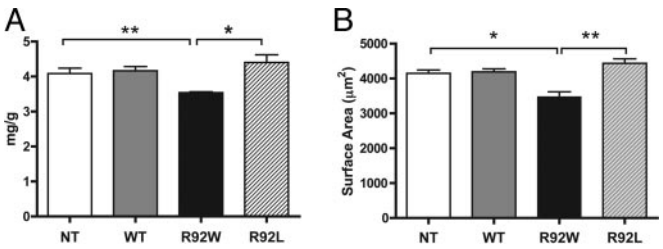

Fig. 3. Mutation-specific alterations in ventricular mass and myocyte size. (*A*) Heart weight/body weight measurements. n = 9, 6, 6, and 8 hearts, respectively. (*B*) Isolated adult cardiac myocyte surface area. n = 71, 52, 29, and 89 cells, respectively. All values are expressed as mean ± SEM. *, $P < 0.01$; **, $P < 0.005$.

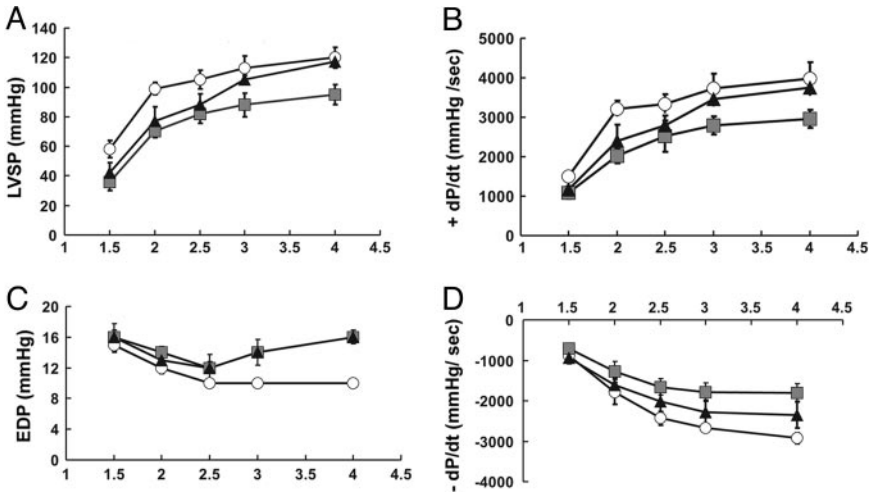

Fig. 4. cTnT R92 mutant hearts exhibit systolic and diastolic dysfunction. (*A* and *B*) Systolic performance: LVSP and the rate of pressure development (+dP/dt) were abnormally low for hearts with either R92 mutation in response to increasing [Ca^{2+}]; the extent of dysfunction for R92W hearts was greater. Both R92W and R92L hearts developed less LVSP at low [Ca^{2+}]. Note that R92L hearts reached a similar LVSP as NT hearts only at high [Ca^{2+}]. (*C* and *D*) Diastolic performance: Hearts with either R92 mutation showed increased end-diastolic pressure (EDP) at high perfusate [Ca^{2+}]. Hearts with a mutation also had slower rates of relaxation (−dP/dt), with R92W ≪ R92L. NT, circles; R92W, squares; R92L, triangles; $n = 4$, for all lines studied.

lines, with the R92W hearts exhibiting a pronounced inability to increase their rate of relaxation in response to increased perfusate [Ca^{2+}] (Fig. 4 *C* and *D*). R92W hearts were also less able to increase developed pressure upon inotropic challenge, which is the case even when developed pressure is normalized by cardiac mass (Fig. 7, which is published as supporting information on the PNAS web site).

Residue 92 Mutations Lead to Early Differential Activation of Pathogenic Signaling Pathways in the Heart. Cardiovascular remodeling is characterized by the activation of complex signaling pathways. To determine whether the independent alterations in cTnT structure caused by the R92W and R92L mutations could induce distinct downstream transcriptional activation patterns, Northern blot analysis was performed on total RNA isolated from ventricular tissue at three time points as shown. Fig. 5*A* shows both representative sibling hearts and Northern blot analyses from sex- and age-matched groups of mutant cTnT mice. Induction of ANF and αSK expression was first detected at 2 months of age in the R92W mice and progressively increased to a peak of 20-fold by 6 months of age followed by a plateau or decrease by 12 months. In addition, there is early activation of the nuclear factor of activated T cells–calcineurin axis in R92W mice as indicated by the 6-fold induction of the Dscr1 gene (encoding MCIP1) (Fig. 4*B*) (23, 24). It is important to note that the early and robust activation of the fetal gene or "hypertrophic" gene program in the R92W mice not only did not lead to overt ventricular hypertrophy, but these hearts (and their myocytes) were smaller than sibling NT mouse hearts. In contrast, the R92L mice did not exhibit any significant induction of the hypertrophic gene program until late adulthood (≈10 months of age), and the late remodeling process in these animals caused a distinct cardiomyopathy characterized by severe biatrial enlargement and a significant decrease in ventricular compliance. Thus, one consequence of different protein structures that result from amino acid substitutions at residue 92 of cTnT is a change in the temporal induction pattern of genes involved in cardiac remodeling. These results show that alterations in the physical properties of a single protein result in perturbations of the complex gene networks controlling cardiac growth and regulation.

Discussion

That structure implies function has long been a central tenet of biochemistry and biophysics in the study of single molecules. The extension of such concepts to protein complexes and alterations that cause disease is as yet unproven. The present study shows that the substitution of either trytophan (R92W) or leucine (R92L) for the native arginine at residue 92 of cTnT leads to distinct phenotypes both at the level of protein conformation and dynamics and when assembled into myofilaments, myocytes, and intact hearts.

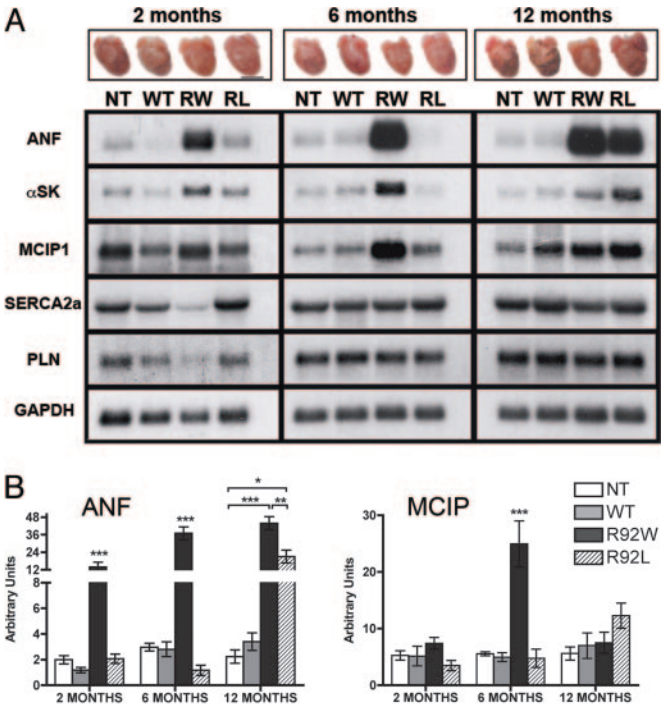

Fig. 5. Mutation-specific temporal activation of cardiomyopathic markers and representative gross hearts. (*A*) Male WT, R92W (RW), R92L (RL), and NT mice were killed at 2-, 6-, and 12-month time points; representative hearts from each time point are shown immediately above the appropriate lane on the Northern blot. Probes were ANF, αSK, MCIP1, sarco(endo)plasmic reticulum calcium ATPase 2a (SERCA2a), phospholamban (PLN), and GAPDH. Each experiment was performed on three independent hearts. (*B*) Quantitation of ANF and MCIP1 transcript levels. Values are shown as ±SEM. *, $P < 0.05$; **, $P < 0.01$; ***, $P < 0.001$.

The R92W cTnT mutation leads to a more severe cardiomyopathy than the R92L cTnT mutation: Hearts with R92W cTnT are smaller and have more prevalent morphological abnormalities, earlier and more fulminant expression of pathogenic markers, and more severe defects in both systolic and diastolic contractile performance. These results support the hypothesis that closely related changes in cTnT structure can result in distinct cardiovascular phenotypes *in vivo* and provide a biophysical basis for the phenotypic variation seen in human FHC.

The thin filament is a multimeric structure that plays both Ca^{2+}-dependent and independent regulatory roles in myofilament activation. The troponin ternary complex modulates the Ca^{2+} dependence of muscle contraction by coupling the level of cytoplasmic Ca^{2+} to the production of mechanical force. cTnT contains two specific functional domains, the Ca^{2+}-independent TnT1 (N-terminal "tail") and the Ca^{2+}-dependent TnT2 domain. Recent biophysical studies have used several of the known FHC cTnT mutations to demonstrate that structural alterations within and immediately flanking the N-terminal tail differentially alter cTnT flexibility and the stability of the TnT–tropomyosin complex (10, 11). Others have suggested that the flexibility of the elongated cTnT N-terminal tail domain is crucial to normal function within the multisubunit troponin complex (25). The region that we study cannot be crystallized and diffracted, likely due to the inherent flexibility found in this region of the TnT (20). Changes in flexibility for the single subdomain of TnT were directly observable in our MD simulation and, to our knowledge, represent the first analytical confirmation of this oft-proposed property. Our simulations demonstrate that this flexibility is subtly affected by single point mutations, showing careful evolutionary control of this property.

Thus, our basic hypothesis for the present study is that observed alterations in the flexibility of the N-terminal tail domain of the mutant cTnT proteins represent discrete and independent changes in cTnT structure/function that initiate specific cascade(s) of downstream myocellular events and eventual cardiac remodeling. One potential mechanism to explain the observed differential remodeling would involve impaired cTnT incorporation. Confocal localization studies of mutant cTnT in R92L and R92W hearts revealed thin filament staining patterns that were indistinguishable from WT. In addition, extensive confocal analysis of several Z band-associated structural proteins (α-actinin, calsarcin 1, and cypher/ZASP) did not reveal evidence of scaffolding disarray (data not shown). Finally, total cTnT amounts were unchanged in both mutant lines compared with NT sibling mice. Taken together, these results suggest that the mutant cTnT proteins incorporate into the native sarcomere and do not cause disease by means of haploinsufficiency. Direct assessment of the structural integrity of the mutant cTnT sarcomeres by means of electron microscopy revealed that both of the cTnT mutant lines exhibited varying degrees of mild myofibrillar lysis that is similar to that seen in hypertrophic cardiomyopathy (26, 27). Neither the R92W nor R92L mutations, however, caused overt sarcomeric disruption or Z band misregistration. Interestingly, our previous studies of a closely related cTnT mutation, Arg-92-Gln (R92Q), revealed widespread lipid deposition consistent with a chronic increase in O_2 demand caused by an increase in the energy cost of force production (19). These changes were not observed in the R92W or R92L sections and demonstrate the sensitivity of the N-terminal tail domain to mutation, suggesting that the R92 alleles cause disease by means of a discrete modulation of thin filament function and subsequent effects on myocellular physiology, not overt sarcomeric disruption.

Cardiac muscle fibers containing many of the FHC-linked mutant cTnT proteins have consistently demonstrated an increase in the Ca^{2+} sensitivity of tension development (13, 18, 28, 29). Despite this high degree of experimental concordance, the mechanistic link between a decrease in the threshold for the Ca^{2+} activation of contraction and the observed clinical phenotype remains unclear. We recently showed that R92W and R92L fibers obtained from the transgenic mice described here exhibited large increases in the pCa [$-$(log [Ca^{2+}])]–tension relationship at both short and long sarcomere lengths compared with WT fibers (30). In addition, no changes in the length dependence of Ca^{2+} sensitivity or the tension-dependent ATP consumption were noted for either R92W or R92L. The differences in magnitude between the R92W and R92L fibers for the Ca^{2+}-dependent parameters were surprisingly small and do not account for the observed mutation-specific phenotypes described here.

Although the direct effects of the R92W and R92L alleles on cardiac ultrastructure and the Ca^{2+} sensitivity of myofilament activation were similar, the mutation-specific downstream effects on cellular and ventricular size and function were strikingly different. The relationship between cardiac size and disease prognosis in hypertrophic cardiomyopathy is a complex and central issue (31). Studies using myosin isolated from an R403Q myosin heavy-chain mouse model of FHC revealed an acceleration in the actin-activating cycling kinetics and an increase in the energy cost of tension development in whole hearts (32, 33). Although these results have led to the hypotheses that the observed clinical hypertrophy in FHC is an adaptive response to an increase in energy demand and/or contractile force at the molecular level, the mechanism that underlies this potential link to the hypertrophic response remains unknown. We have recently shown that this proposed mechanism does not apply to the cTnT R92Q mutation, where the observed energetic deficits did not lead to ventricular hypertrophy (19). The results presented here for two closely related mutations, R92W and R92L, show that the smaller hearts had worse contractile performance. Thus, we propose that the important property common to both myosin heavy-chain and cTnT mutant hearts is not hypertrophy *per se* but abnormal thick filament–thin filament interactions sufficient to directly impair systolic and diastolic performance.

The R92W and R92L mutations in cTnT exhibit divergent ventricular remodeling patterns in patients and in mice and thus represent a unique model system to investigate the link(s) between contractile dysfunction at the molecular level and abnormal cardiac growth in FHC. The observed 14% decrease in ventricular mass in the R92W mice was consistent with previous findings from our laboratory and others for murine models of cTnT-related FHC (15, 16, 22). In contrast, the R92L mice developed a mild ventricular hypertrophy (a 23% increase in ventricular mass when compared with the R92W mice). These differences were apparent at both the whole-heart and single myocyte levels as early as 1 month of age (data not shown), suggesting that the alterations in myocyte growth are an early component of the differential pathogenic response to the cTnT mutations.

The development of cardiac hypertrophy has long been an active area of investigation, recently reviewed in ref. 34. Recently, attention has been focused on myocellular signaling pathways that act to sense the physiologic demands on the myocardium by means of membrane-bound receptor molecules and eventually result in growth and remodeling-related transcriptional activation (mechanotransduction). One of the difficulties in studying the pathogenesis of cardiomyopathies lies in the inherent multifactoral and progressive myocellular response to physiologic stress. In particular, the pathways that transduce primary alterations in contractility at the level of the sarcomere to transcriptional activation remain unclear. An advantage of the current model system is that the "stressors" (cTnT mutations) are intrinsic to the sarcomere and thus may eventually serve to identify the mechanisms involved.

One potential link between the mutation-specific alterations in cTnT structure/function and the divergent ventricular remodeling involves the differential activation of Z band-associated signaling pathways (35). For example, the Ca^{2+}-activated protein phosphatase calcineurin has been linked to the activation of the fetal gene program (including ANF) and the subsequent development of pathologic cardiac hypertrophy by means of its downstream effec-

tor, nuclear factor of activated T cells (NFAT). Calcineurin is localized to the sarcomeric Z band in cardiac myocytes and is activated by means of sustained increases in intracellular calcium; it is thus uniquely positioned to serve as a potential sensor of thin filament dysfunction. Because direct measurement of calcineurin activity has led to conflicting reports, here we probed for the expression of the calcineurin inhibitor MCIP1, which has been shown to be induced in response to calcineurin activation (36). Significant (5-fold) MCIP1 induction was observed only at the 6-month time point in R92W mice and, unlike ANF, was not sustained. These findings suggest that, although the calcineurin–NFAT axis is significantly activated in the R92W hearts, it is not likely to be part of the primary process and may instead represent a secondary response to the initial stimulus. Other known Z band/thin filament-associated binding molecules (calsarcin 1, cypher/ZASP, and α-actinin) did not exhibit any alterations in mRNA transcript levels or delocalization from the Z band (data not shown). We also did not detect any significant changes in the sarco(endo)plasmic reticulum calcium ATPase 2a/phospholamban ratio at the transcript level at any time point.

One important finding shown here is that, although the overall magnitude of ANF and αSK induction for both R92W and R92L was similar, the timing of the transcriptional activation differed. Comparison of the representative hearts at each time point shows that the progression of the ventricular remodeling is also divergent, with the R92W hearts appearing to undergo an early growth "arrest" that is first apparent at 2 months of age. A similar robust induction of the fetal gene program in the absence of overt ventricular hypertrophy was recently reported for the calsarcin 1 knockout mouse, suggesting that the activation of the fetal gene program and the development of ventricular hypertrophy can be uncoupled *in vivo* (37). In contrast, the induction of the fetal gene program was not detectable until 10 months of age in the R92L mice that developed a late onset, mild to moderate concentric hypertrophy. This surprising result suggests that a major determinant of the observed differential remodeling is the timing of the initial pathogenic response.

In summary, R92W and R92L missense mutations in cTnT lead to alterations in protein flexibility and the subsequent development of mutation-specific cardiovascular phenotypes by means of activation of discrete pathways leading to ventricular remodeling. Although we have not defined the precise chemical links between a change in the flexibility of the mutant cTnT proteins and the activation of discrete cardiomyopathic signaling pathways, it is clear that within this highly controlled *in vivo* system, the final complex phenotypes are in part due to discrete changes in thin filament structure at the level of the cardiac sarcomere. Phenotypic variation has recently led some investigators to question whether genotype determination in FHC is a worthwhile adjunct to determining risk and eventual prognosis (38). Our results suggest that it is worthwhile. Our data strongly support the hypothesis that discrete changes in the biophysical properties of the sarcomeric proteins caused by single amino acid mutations lead directly to the activation of signaling pathways that alter both the time of onset and the degree of ventricular remodeling. Although it is always difficult to extrapolate from murine models to complex cardiac diseases, it is important to note that the disease onset for patients with the R92W (early and severe) and R92L (late and moderate) mutations is fully recapitulated in our murine models, which should be useful in identifying potential therapeutic approaches to alter the natural history of the disease. The findings presented in this study, coupled with our previous observations of impaired contractile reserve and energetics, reaffirm the original hypothesis that FHC is a primary disease of the cardiac sarcomere.

We thank Yvonne Kress (Albert Einstein College of Medicine) for invaluable assistance with electron microscopy. This work was supported by National Institutes of Health Grants K08 HL68619 and R01 HL075619 (to J.C.T.) and HL052320, HL063985, and HL075619 (to J.S.I.).

1. Tobacman, L. S. (1996) *Annu. Rev. Physiol.* **58,** 447–481.
2. Li, M. X., Wang, X. & Sykes, B. D. (2004) *J. Muscle Res. Cell Motil.* **25,** 559–579.
3. Watkins, H., McKenna, W. J., Thierfelder, L., Suk, H. J., Anan, R., O'Donoghue, A., Spirito, P., Matsumori, A., Moravec, C. S., Seidman, J. G. & Seidman, C. E. (1995) *N. Engl. J. Med.* **332,** 1058–1064.
4. Forissier, J. F., Carrier, L., Farza, H., Bonne, G., Bercovici, J., Richard, P., Hainque, B., Townsend, P. J., Yacoub, M. H., Faure, S., *et al.* (1996) *Circulation* **94,** 3069–3073.
5. Elliott, P. M., Sharma, S., Varnava, A., Poloniecki, J., Rowland, E. & McKenna, W. J. (1999) *J. Am. Coll. Cardiol.* **33,** 1596–1601.
6. Kamisago, M., Sharma, S. D., DePalma, S. R., Solomon, S., Sharma, P., McDonough, B., Smoot, L., Mullen, M. P., Woolf, P. K., Wigle, E. D., *et al.* (2000) *N. Engl. J. Med.* **343,** 1688–1696.
7. Moolman, J. C., Corfield, V. A., Posen, B. M., Ngumbela, K., Seidman, C. E., Brink, P. A. & Watkins, H. (1997) *J. Am. Coll. Cardiol.* **29,** 549–555.
8. Hinkle, A., Goranson, A., Butters, C. A. & Tobacman, L. S. (1999) *J. Biol. Chem.* **274,** 7157–7164.
9. Tobacman, L. S., Nihli, M., Butters, C., Heller, M., Hatch, V., Craig, R., Lehman, W. & Homsher, E. (2002) *J. Biol. Chem.* **277,** 27636–27642.
10. Palm, T., Graboski, S., Hitchcock-DeGregori, S. E. & Greenfield, N. J. (2001) *Biophys. J.* **81,** 2827–2837.
11. Hinkle, A. & Tobacman, L. S. (2003) *J. Biol. Chem.* **278,** 506–513.
12. Tobacman, L. S., Lin, D., Butters, C., Landis, C., Back, N., Pavlov, D. & Homsher, E. (1999) *J. Biol. Chem.* **274,** 28363–28370.
13. Harada, K. & Potter, J. D. (2004) *J. Biol. Chem.* **279,** 14488–14495.
14. Brooks, B. R., Bruccolerii, R. E., Olafson, B. D., States, D. J., Swaminathan, S. & Karplus, M. (1983) *J. Comput. Chem.* **4,** 187–217.
15. Tardiff, J. C., Hewett, T. E., Palmer, B. M., Olsson, C., Factor, S. M., Moore, R. L., Robbins, J. & Leinwand, L. A. (1999) *J. Clin. Invest.* **104,** 469–481.
16. Tardiff, J. C., Factor, S. M., Tompkins, B. D., Hewett, T. E., Palmer, B. M., Moore, R. L., Schwartz, S., Robbins, J. & Leinwand, L. A. (1998) *J. Clin. Invest.* **101,** 2800–2811.
17. Nagata, K., Liao, R., Eberli, F. R., Satoh, N., Chevalier, B., Apstein, C. S. & Suter, T. M. (1998) *Cardiovasc. Res.* **37,** 467–477.
18. Montgomery, D. E., Tardiff, J. C. & Chandra, M. (2001) *J. Physiol.* **536,** 583–592.
19. Javadpour, M. M., Tardiff, J. C., Pinz, I. & Ingwall, J. S. (2003) *J. Clin. Invest.* **112,** 768–775.
20. Takeda, S., Yamashita, A., Maeda, K. & Maeda, Y. (2003) *Nature* **424,** 35–41.
21. Hughes, S. E. & McKenna, W. J. (2005) *Heart* **91,** 257–264.
22. Miller, T., Szczesna, D., Housmans, P. R., Zhao, J., de Freitas, F., Gomes, A. V., Culbreath, L., McCue, J., Wang, Y., Xu, Y., *et al.* (2001) *J. Biol. Chem.* **276,** 3743–3755.
23. Rothermel, B., Vega, R. B., Yang, J., Wu, H., Bassel-Duby, R. & Williams, R. S. (2000) *J. Biol. Chem.* **275,** 8719–8725.
24. Vega, R. B., Rothermel, B. A., Weinheimer, C. J., Kovacs, A., Naseem, R. H., Bassel-Duby, R., Williams, R. S. & Olson, E. N. (2003) *Proc. Natl. Acad. Sci. USA* **100,** 669–674.
25. Greenfield, N. J., Palm, T. & Hitchcock-DeGregori, S. E. (2002) *Biophys. J.* **83,** 2754–2766.
26. Davies, M. J. & McKenna, W. (1995) *Histopathology* **26,** 493–500.
27. Varnava, A. M., Elliott, P. M., Sharma, S., McKenna, W. J. & Davies, M. J. (2000) *Heart* **84,** 476–482.
28. Yanaga, F., Morimoto, S. & Ohtsuki, I. (1999) *J. Biol. Chem.* **274,** 8806–8812.
29. Redwood, C., Lohmann, K., Bing, W., Esposito, G. M., Elliott, K., Abdulrazzak, H., Knott, A., Purcell, I., Marston, S. & Watkins, H. (2000) *Circ. Res.* **86,** 1146–1152.
30. Chandra, M., Tschirgi, M. L. & Tardiff, J. C. (2005) *Am. J. Physiol.* **289,** H2112–H2119.
31. Maron, M. S., Zenovich, A. G., Casey, S. A., Link, M. S., Udelson, J. E., Aeppli, D. M. & Maron, B. J. (2005) *Am. J. Cardiol.* **95,** 1329–1333.
32. Palmiter, K. A., Tyska, M. J., Haeberle, J. R., Alpert, N. R., Fananapazir, L. & Warshaw, D. M. (2000) *J. Muscle Res. Cell Motil.* **21,** 609–620.
33. Spindler, M., Saupe, K., Christe, M., Sweeney, H. L., Seidman, C. E. & Seidman, J. G. (1998) *J. Clin. Invest.* **101,** 1775–1783.
34. Frey, N. & Olson, E. N. (2003) *Annu. Rev. Physiol.* **65,** 45–79.
35. Wilkins, B. J., Dai, Y. S., Bueno, O. F., Parsons, S. A., Xu, J., Plank, D. M., Jones, F., Kimball, T. R. & Molkentin, J. D. (2004) *Circ. Res.* **94,** 110–118.
36. Rothermel, B. A., Vega, R. B. & Williams, R. S. (2003) *Trends Cardiovasc. Med.* **13,** 15–21.
37. Frey, N., Barrientos, T., Shelton, J. M., Frank, D., Rutten, H., Gehring, D., Kuhn, C., Lutz, M., Rothermel, B., Bassel-Duby, R., *et al.* (2004) *Nat. Med.* **10,** 1336–1343.
38. Ackerman, M. J. (2005) *Curr. Opin. Cardiol.* **20,** 175–181.